Fast Layout-Oblivious Tensor-Matrix Multiplication with BLAS

Cem Bassoy

Hamburg University of Technology, Schwarzenbergstrasse 95, Germany,
`cem.bassoy@gmail.com`

Abstract. The tensor-matrix product is a compute-bound tensor operations and required in various tensor methods, e.g. for computing the ALS or HOSVD. This paper presents a high-performance algorithm for the mode-q tensor-matrix multiplication using the Loops-over-`GEMM`s (`LOG`) approach with dense tensors that can have any linear tensor layout, tensor order and dimensions. The proposed algorithm either directly calls efficient implementations of `GEMM` with tensors or recursively apply `GEMM` on higher-order tensor slices multiple times. We discuss different strategies for fusing and executing the matrix-matrix multiplication in parallel. Using `OpenBLAS`, our parallel implementation attains [**?**] Gflops/s in single precision on a Core i9-7900X Intel Xeon processor. We show that the performance of our implementation is independent of the tensor layout and a performance of [**?**] can be sustained for any linear tensor format. Our version of the tensor-matrix multiplication is on average [**?**] x and up to [**?**] x faster than state-of-the-art approaches.

1 Introduction

Tensor computations are found in many scientific fields such as computational neuroscience, pattern recognition, signal processing and data mining [7,14]. Tensors representing large amount of multidimensional data are decomposed and analyzed with the help of basic tensor operations [8,9]. The decomposition and analysis led to the development and analysis of high-performance kernels for tensor contractions. In this work, we present and analyze a high-performance algorithm for the tensor-matrix multiplication that is used in many numerical algorithms such as the alternating least squares method [8,9]. It is a compute-bound tensor operation and has the same arithmetic intensity as a matrix-matrix multiplication which can reach near peak performance of a computing machine.

To our best knowledge, there has been three main approach to implement tensor contractions. The Transpose-Transpose-`GEMM`-Transpose (`TGGT`) approach reorganizes (flatens) tensors in order to perform a tensor contraction with an optimized matrix-matrix multiplication (`GEMM`) implementation [2,16]. Implementations of a more recent method (`GETT`) are based on high-performance `GEMM`-like algorithms [1,12,17]. A different method is the `LOG` approach in which algorithms utilize `GEMM` with multiple tensor slices if possible [10,13,15].

Our analysis is motivated by the observation that `LOG` implementations of the tensor-matrix multiplication has not been fully thoroughly investigated. Our approach is akin to the one proposed in [10,15] but targets the utilization of general matrix-matrix multiplication routines (`GEMM`) using `OpenBLAS`, `Intel MKL` and `BLIS` without code generation. The recursive in-place algorithms is similar to the one presented in [3] and computes the tensor-matrix multiplication by executing `GEMM` with slices and fibers of tensors. However, the presented algorithm requires twice as many cases and has also additional implementation options which has not been previously discussed. Moreover, except for few corner cases, we demonstrate that our algorithm is able to perform the multiplication with any contraction mode using multiple slice-matrix multiplications and only one `GEMM` parameter configuration. For parallel execution, we propose a variable loop fusion method with respect to the slice order of slice-vector multiplications. Our algorithms support dense tensors with any order, dimensions and any linear tensor layout including the first- and the last-order storage formats for any contraction mode. We have quantified the impact of the tensor layout, tensor slice order and parallel execution of slice-matrix multiplications with varying contraction modes. The runtime measurements of our implementations are compared with those presented in [1, 12, 17]. In summary, the main findings of our work are:

- A tensor-matrix multiplication is implementable by an in-place algorithm with 1 `GEMV` and 7 `GEMM` parameter configurations supporting all combinations of contraction mode, tensor order and dimensions.
- Algorithms with variable loop fusion and parallel slice-matrix multiplications can achieve the peak performance of a `GEMM` with large slice dimensions. Moreover, the proposed algorithm is layout oblivious and is able to achieve a sustainable performance throughput for any linear tensor layout.
- A `LOG`-based tensor-times-matrix implementation can be faster than `TTGT`- and `GETT`-based implementations that have been described in [12, 17]. Using symmetrically shaped tensors, an average speedup of [**?**] x to [**?**] x for single and double precision floating point computations can be achieved.

The remainder of the paper is organized as follows. Section 2 presents related work. Section 3 introduces the terminology used in this paper and defines the tensor-vector multiplication. Algorithm design and methods for parallel execution is discussed in Section 4. Section 5 describes the test setup and discusses the benchmark results in Section 6. Conclusions are drawn in Section 7.

2 Related Work

The authors in [13] discuss the efficient tensor contractions with highly optimized `BLAS`. Based on the `LOG` approach, they define requirements for the use of `GEMM` for class 3 tensor contractions and provide slicing techniques for tensors. The slicing recipe for the class 2 categorized tensor contractions contains a short description

with a rule of thumb for maximizing performance. Runtime measurements cover class 3 tensor contractions.

The work in [10] presents a framework that generates in-place tensor-matrix multiplication according to the LOG approach. The authors present two strategies for efficiently computing the tensor contraction applying GEMMs with tensors. They report a speedup of up to 4x over the TTGT-based MATLAB tensor toolbox library discussed in [2]. Although many aspects are similar to our work, the authors emphasize the code generation of tensor-matrix multiplications using high-performance GEMM's.

The authors of [17] present a tensor-contraction generator TCCG and the GETT approach for dense tensor contractions that is inspired from the design of a high-performance GEMM. Their unified code generator selects implementations from generated GETT, LoG and TTGT candidates. Their findings show that among 48 different contractions 15% of LoG based implementations are the fastest. However, their tests do not include the tensor-vector multiplication where the contraction exhibits at least one free tensor index.

Using also the GETT approach, the author presents in [12] a runtime flexible tensor contraction library. He describes block-scatter-matrix algorithm which uses a special layout for the tensor contraction. The proposed algorithm yields results that feature a similar runtime behavior to those presented in [17].

3   Background

Notation An order-p tensor is a p-dimensional array [11] where tensor elements are contiguously stored in memory. We write a, $\mathbf{a}$, $\mathbf{A}$ and $\underline{\mathbf{A}}$ in order to denote scalars, vectors, matrices and tensors. In general we assume a tensor $\underline{\mathbf{A}}$ to have a tensor order with $p > 2$. The p-tuple $\mathbf{n}$ with $\mathbf{n} = (n_1, n_2, \ldots, n_p)$ will be referred to as a dimension tuple with $n_r > 1$. We will use round brackets $\underline{\mathbf{A}}(i_1, i_2, \ldots, i_p)$ or $\underline{\mathbf{A}}(\mathbf{i})$ to denote a tensor element where $\mathbf{i} = (i_1, i_2, \ldots, i_p)$ is a multi-index.

A subtensor denoted by $\underline{\mathbf{A}}'$ references a subset of tensor elements. The subtensor elements are specified with p index ranges and form a selection grid. The r-th index range shall be given by an index pair denoted by $f_r : l_r$ with $1 \leq f_r \leq l_r \leq n_r$ with $l_r - f_r + 1 = n'_r$. A subtensor is called a slice $\underline{\mathbf{A}}'_{u,v}$ if two modes $1 \leq u \neq v \leq p$ of the corresponding tensor $\underline{\mathbf{A}}$ are selected with a full index range. The remaining modes are selected with a single index so that only two dimensions of the slice are greater than one. A fiber $\underline{\mathbf{A}}'_u$ is a tensor slice with only one dimension greater than 1.

Linear Tensor Layouts We use a layout tuple $\boldsymbol{\pi} \in \mathbb{N}^p$ to encode all linear tensor layouts including the first-order or last-order layout. They contain permuted tensor modes whose priority is given by their index. For instance, the first- and last-order storage formats are given by $\boldsymbol{\pi}_F = (1, 2, \ldots, p)$ and $\boldsymbol{\pi}_L = (p, p-1, \ldots, 1)$. An inverse layout tuple $\boldsymbol{\pi}^{-1}$ is defined by $\boldsymbol{\pi}^{-1}(\boldsymbol{\pi}(k)) = k$. Given a layout tuple $\boldsymbol{\pi}$ with p modes, the π_r-th element of a stride tuple is given

by $w_{\pi_r} = \prod_{k=1}^{r-1} n_{\pi_k}$ for $1 < r \leq p$ and $w_{\pi_1} = 1$. Tensor elements of the π_1-th mode are contiguously stored in memory.

The location of tensor elements within the allocated memory space is determined by the tensor layout and the corresponding layout function. For a given layout and stride tuple, a layout function $\lambda_{\mathbf{w}}$ maps a multi-index to a scalar index with $\lambda_{\mathbf{w}}(\mathbf{i}) = \sum_{r=1}^{p} w_r(i_r - 1)$. With $j = \lambda_{\mathbf{w}}(\mathbf{i})$ being the relative memory position of an element with a multi-index $\mathbf{i}$, reading from and writing to memory is accomplished with j and the first element's address of $\underline{\mathbf{A}}$.

Flattening and Reshaping The flattening operation $\varphi_{r,q}$ transforms an order-p tensor $\underline{\mathbf{A}}$ to another order-p' tensor $\underline{\mathbf{B}}$ with different shape $\mathbf{m}$ and layout $\boldsymbol{\tau}$ tuples of length p' with $p' = p - q + r$ and $1 \leq r < q \leq p$. It is related to the tensor unfolding operation as defined in [8, p.459] but does neither change the element ordering nor copies tensor elements. Given a layout tuple $\boldsymbol{\pi}$ of $\underline{\mathbf{A}}$, the flattening operation $\varphi_{r,q}$ is defined for contiguous modes $\boldsymbol{\pi}_{r,q} = (\pi_r, \pi_{r+1}, \ldots, \pi_q)$ of $\boldsymbol{\pi}$. Let $s = 0$ if $\pi_r < \max(\boldsymbol{\pi}_{r,q})$ and $s = q - r$ if $\pi_k > \max(\boldsymbol{\pi}_{r,q})$ for $1 \leq k \neq r \leq p'$. Let $j = 0$ if $k < r$ and $j = q - r$ if $k > r$, then the resulting layout tuple $\boldsymbol{\tau} = (\tau_1, \ldots, \tau_{p'})$ of $\underline{\mathbf{B}}$ is given by $\tau_r = \min(\boldsymbol{\pi}_{r,q})$ and $\tau_{k+j} = \pi_k + s$ for $k \neq r$. Elements of the corresponding shape tuple $\mathbf{m}$ are given by $\mathbf{m}(\tau_r) = \prod_{k=r}^{q} \mathbf{n}(\pi_k)$ and $\mathbf{m}(\tau_k) = \mathbf{n}(\pi_{k+j})$ where $j = 0$ if $k < r$ and $j = q - r$ if $k > r$.

The reshaping operation ρ transforms an order-p tensor $\underline{\mathbf{A}}$ to another order-p tensor $\underline{\mathbf{B}}$ with different shape $\mathbf{m}$ and layout $\boldsymbol{\tau}$ tuples of length p. In this work, it permutes the shape and layout tuple simultaneously without changing the element ordering. Given the permutation tuple $\boldsymbol{\rho} = (\rho_1, \ldots, \rho_p)$ defining the reshaping operation, the resulting shape tuple $\mathbf{m}$ of $\mathbf{n}$ and the layout tuple $\boldsymbol{\tau}$ are given by $m_r = \mathbf{n}(\rho_r)$ and $\tau_r = \boldsymbol{\pi}(\rho_r)$, respectively.

Tensor-Matrix Multiplication (TTM) Let $\underline{\mathbf{A}}$ and $\underline{\mathbf{C}}$ be order-p tensors with shapes $\mathbf{n}_a = (n_1, \ldots, n_q, \ldots, n_p)$ and $\mathbf{n}_c = (n_1, \ldots, n_{q-1}, m, n_{q+1}, \ldots, n_p)$. Let $\mathbf{B}$ be a matrix of shape $\mathbf{n}_b = (m, n_q)$. A mode-q TTM is denoted by $\underline{\mathbf{C}} = \underline{\mathbf{A}} \times_q \mathbf{B}$ where an element of $\underline{\mathbf{C}}$ is given by

$$\underline{\mathbf{C}}(i_1, \ldots, i_{q-1}, j, i_{q+1}, \ldots, i_p) = \sum_{i_q=1}^{n_q} \underline{\mathbf{A}}(i_1, \ldots, i_q, \ldots, i_p) \cdot \mathbf{B}(j, i_q) \qquad (1)$$

with $1 \leq i_r \leq n_r$ and $1 \leq j \leq m$. The mode q is the *contraction mode* of the TTM with $1 \leq q \leq p$. The tensor-matrix multiplication generalizes the computational aspect of the two-dimensional case $\mathbf{C} = \mathbf{B} \cdot \mathbf{A}$ if $p = 2$ and $q = 1$. Its arithmetic intensity is equal to that of a matrix-matrix multiplication and is not memory-bound. In the following, we assume that the tensors $\underline{\mathbf{A}}$ and $\underline{\mathbf{C}}$ have the same tensor layout $\boldsymbol{\pi}$. Elements of matrix $\underline{\mathbf{B}}$ can stored in either the column-major or row-major format.

4 Algorithm Design

4.1 Sequential Baseline Algorithm

The sequential baseline algorithm implementing Eq. 1 can be implemented with a single C++ function. It consists of nested recursion with a control flow that resembles algorithm 1 in [4], consisting of two `if` statements with an `else` branch. The body of the first `if` statement contains a recursive call that skips the iteration over the dimension n_q when $r = \hat{q}$ with $\pi_r = q$ and $\hat{q} = \boldsymbol{\pi}_q^{-1}$ where $\boldsymbol{\pi}^{-1}$ is the inverse layout tuple. The second `if` statement contains multiple recursive calls for the modes $1 \leq r \neq \hat{q} \leq p$ with different multi-indices. Note that the second `if` statement is skipped for $q = \pi_1$ as the condition of the first one is evaluated to true. The `else` branch is the base case and consists of two loops that compute a fiber-matrix product. The inner loop iterates over the dimension n_q of $\underline{\mathbf{A}}$ and $\mathbf{B}$ with index $1 \leq i_q \leq n_q$ computing an inner product. The outer loop iterates over the dimension m of $\underline{\mathbf{C}}$ and $\mathbf{B}$ with index $1 \leq j \leq m$. The baseline algorithm supports tensors with arbitrary order, dimensions and any non-hierarchical storage format.

4.2 Modified Baseline Algorithm with Contiguous Memory Access

The baseline algorithm accesses memory of $\underline{\mathbf{A}}$ and $\underline{\mathbf{C}}$ non-contiguously whenever $\pi_1 \neq q$ so that indices i_q and j are incremented with steps greater than one. Matrix $\mathbf{B}$ is contiguously accessed if i_q or j is incremented with unit-steps depending on the storage format of $\underline{\mathbf{B}}$. The access pattern could be improved by reordering tensor elements according to the storage format which results in copy operations reducing the overall throughput of the operation [15].

A better approach is to access tensor elements according to the tensor layout using the permutation tuple $\boldsymbol{\pi}$ as proposed in [4]. The modified algorithm with contiguous memory accesses is given in algorithm 1 for $\pi_1 \neq q$ and $p > 1$. Each recursion level adjusts only one multi-index element $\mathbf{i}(\pi_r)$ with a stride $\mathbf{w}(\pi_r)$ as depicted in line 5. With increasing recursion level and decreasing r, indices are incremented with smaller step sizes as $\mathbf{w}(\pi_r) \leq \mathbf{w}(\pi_{r+1})$. The condition of the second `if` statement in line 4 is changed from $r \geq 1$ to $r > 1$. In this way, the loop incrementing with index $\mathbf{i}(\pi_1)$ and the minimum stride $\mathbf{w}(\boldsymbol{\pi}_1)$ can be included in the base case which contains three loops performing a slice-matrix multiplication. The ordering of the three loops within the base case are adjusted according to the tensor and matrix layout. The inner-most loop increments $\mathbf{i}(\pi_1)$ and therefore contiguously accesses tensor elements of $\underline{\mathbf{A}}$ and $\underline{\mathbf{C}}$. The second loop increments i_q with which elements of $\mathbf{B}$ are contiguously accessed if $\mathbf{B}$ is stored in the row-major format. The third loop increments j and could be placed as the second loop if $\mathbf{B}$ is stored in the column-major format. The simple ordering of the three loops is discussed in [5].

While the spatial data locality is improved by adjusting the loop ordering, the temporal data locality of tensors $\underline{\mathbf{A}}$ and $\underline{\mathbf{C}}$ differ. Note that slice $\underline{\mathbf{A}}'_{\pi_1,q}$ is accessed m times, fiber $\underline{\mathbf{C}}_{\pi_1}$ is accessed $\mathbf{n}(q)$ times and element $\underline{\mathbf{B}}(j, i_q)$ is accessed $\mathbf{n}(\pi_1)$

```
1  tensor_times_matrix($\underline{\mathbf{A}}, \mathbf{B}, \underline{\mathbf{C}}, \mathbf{n}, \mathbf{i}, m, q, \hat{q}, r$)
2     if $r = \hat{q}$ then
3        tensor_times_matrix($\underline{\mathbf{A}}, \mathbf{B}, \underline{\mathbf{C}}, \mathbf{n}, \mathbf{i}, m, q, \hat{q}, r-1$)
4     else if $r > 1$ then
5        for $i_{\pi_r} \leftarrow 1$ to $n_{\pi_r}$ do
6           tensor_times_matrix($\underline{\mathbf{A}}, \mathbf{B}, \underline{\mathbf{C}}, \mathbf{n}, \mathbf{i}, m, q, \hat{q}, r-1$)
7     else
8        for $j \leftarrow 1$ to $m$ do
9           for $i_q \leftarrow 1$ to $n_q$ do
10             for $i_{\pi_1} \leftarrow 1$ to $n_{\pi_1}$ do
11                $\underline{\mathbf{C}}(i_1, ..., i_{q-1}, j, i_{q+1}, ..., i_p)$ += $\underline{\mathbf{A}}(i_1, ..., i_q, ..., i_p) \cdot \mathbf{B}(j, i_q)$
```

Algorithm 1: Modified baseline algorithm with contiguous memory access for the tensor-matrix multiplication. The tensor order must be greater than one and for the contraction mode $1 \leq q \leq p$ and $\pi_1 \neq q$ must hold. The algorithm needs to be initially called with $r = p$ where $\mathbf{n}$ is the shape tuple of $\underline{\mathbf{A}}$ and m is the q-th dimension of $\underline{\mathbf{C}}$.

times. While the specified fiber of $\underline{\mathbf{C}}$ can fit into first or second level cache, slice elements of $\underline{\mathbf{A}}$ are unlikely to fit in the local caches if the slice size $n_{\pi_1} \times n_q$ is large leading to higher cache misses and suboptimal performance. Optimized tiling for better temporal data locality has been discussed in [6] which suggests to use existing high-performance BLAS implementations for the base case.

4.3 GEMM-based Algorithms

The proposed algorithm 1 is the starting point for the BLAS-based algorithm which computes the tensor-matrix product with a `GEMM` routine. Besides the illustrated algorithm, we have identified seven other cases where a single `GEMM` call suffices to compute the tensor-matrix product even if the tensor order p is greater than two. In summary there are eight cases with a single `GEMM` call using different arguments which are listed in table 1. The table is complete with no limitation on tensor order and contraction mode, supporting all linear tensor layout. `GEMM` arguments are chosen depending on the tensor order p, tensor layout $\boldsymbol{\pi}$ and contraction mode q except for the `CBLAS_ORDER` which is `CblasRowMajor`.

Case 1 ($p = 1$): The tensor-vector product $\underline{\mathbf{A}} \times_1 \mathbf{B}$ can be computed with a `GEMV` operation $\mathbf{a}^T \cdot \mathbf{B}$ where $\underline{\mathbf{A}}$ is an order-1 tensor, i.e. a vector $\mathbf{a}$ of length n_1.

Case 2-5 ($p = 2$): If $\underline{\mathbf{A}}$ and $\underline{\mathbf{C}}$ are order-2 tensors, i.e. a matrix $\mathbf{A}$ with dimensions n_1 and n_2, then a single `GEMM` suffices to compute the tensor-matrix product. If $\mathbf{A}$ and $\mathbf{C}$ have the column-major format with $\boldsymbol{\pi} = (1, 2)$, `GEMM` either executes $\mathbf{C} = \mathbf{A} \cdot \mathbf{B}^T$ for $q = 1$ or $\mathbf{C} = \mathbf{B} \cdot \mathbf{A}$ for $q = 2$. Note that `GEMM` interprets $\mathbf{C}$ and $\mathbf{A}$ as matrices in row-major format even though both are stored column-wise. If $\mathbf{A}$ and $\mathbf{C}$ have the row-major format with $\boldsymbol{\pi} = (2, 1)$, `GEMM` either executes

Case	Order p	Layout $\boldsymbol{\pi}$	Mode q	Routine	T	M	N	K	A	LDA	B	LDB	LDC
1	1	-	1	GEMV	-	m	n_1	-	$\mathbf{B}$	n_1	$\underline{\mathbf{A}}$	-	-
2	2	$(1,2)$	1	GEMM	$\mathbf{B}$	n_2	m	n_1	$\underline{\mathbf{A}}$	n_1	$\mathbf{B}$	n_1	m
3	2	$(1,2)$	2	GEMM	-	m	n_1	n_2	$\mathbf{B}$	n_2	$\underline{\mathbf{A}}$	n_1	n_1
4	2	$(2,1)$	1	GEMM	-	m	n_2	n_1	$\mathbf{B}$	n_1	$\underline{\mathbf{A}}$	n_2	n_2
5	2	$(2,1)$	2	GEMM	$\mathbf{B}$	n_1	m	n_2	$\underline{\mathbf{A}}$	n_2	$\mathbf{B}$	n_2	m
6	>2	any	π_1	GEMM	$\mathbf{B}$	$\bar{n}_q$	m	n_q	$\underline{\mathbf{A}}$	n_q	$\mathbf{B}$	n_q	m
7	>2	any	π_p	GEMM	-	m	$\bar{n}_q$	n_q	$\mathbf{B}$	n_q	$\underline{\mathbf{A}}$	$\bar{n}_q$	$\bar{n}_q$
8	>2	any	$\pi_2,..,\pi_{p-1}$	GEMM*	-	m	n_{π_1}	n_q	$\mathbf{B}$	n_q	$\underline{\mathbf{A}}$	n_{π_1}	n_{π_1}

Table 1. Parameter configuration of the `GEMV`- and `GEMM` routines with eight cases computing a tensor-matrix product. The routine arguments are chosen with respect to the tensor order p, tensor layout $\boldsymbol{\pi}$ and contraction mode q which determine the `GEMM` arguments for `T`, `M` to `LDC`. The parameter `T` denotes the transposition for matrix $\mathbf{B}$. The routine `GEMM*` denotes multiple `GEMM` calls with different tensor slices. The number of rows for case 6 and 7 is given by $\bar{n}_q = \bar{n}/n_q$ with $\bar{n} = n_1 \cdots n_p$.

$\mathbf{C} = \mathbf{B} \cdot \mathbf{A}$ for $q = 1$ or $\mathbf{C} = \mathbf{A} \cdot \mathbf{B}^T$ for $q = 2$. Note that the transposition of $\mathbf{B}$ is necessary for the cases 2,5 and independent of the chosen storage format.

Case 6-7 ($p > 2$): If the order of $\underline{\mathbf{A}}$ and $\underline{\mathbf{C}}$ is greater than 2 and if the contraction mode q is equal to π_1, a single `GEMM` with the depicted parameters executes $\mathbf{C} = \mathbf{A} \cdot \mathbf{B}^T$ and computes a tensor-matrix product $\underline{\mathbf{C}} = \underline{\mathbf{A}} \times_{\pi_1} \mathbf{B}$ for any storage layout of $\underline{\mathbf{A}}$ and $\underline{\mathbf{C}}$. Tensors $\underline{\mathbf{A}}$ and $\underline{\mathbf{C}}$ are flattened to row-major matrices $\mathbf{A}$ and $\mathbf{C}$ using $f_{2,p}$, see subsection **??**. Matrix $\mathbf{A}$ has $\bar{n}_q = \bar{n}/n_q$ rows and n_q columns while matrix $\mathbf{C}$ has the same number of rows and m columns. If $\pi_p = q$, the `GEMM` executes $\mathbf{C} = \mathbf{B} \cdot \mathbf{A}$ and computes a tensor-matrix product $\underline{\mathbf{C}} = \underline{\mathbf{A}} \times_{\pi_p} \mathbf{B}$ for any storage layout of $\underline{\mathbf{A}}$ and $\underline{\mathbf{C}}$. The matrix $\mathbf{A}$ has n_q rows and $\bar{n}_q$ rows while matrix $\mathbf{C}$ has m rows and the same number of columns. Note that in all cases no copy operation is performed in order to compute the desired contraction.

Case 8 ($p > 2$): If the tensor order is greater than 2, $\pi_1 \neq q$ and $\pi_p \neq q$, the modified baseline algorithm 1 is used to successively call $\bar{n}/(n_q \cdot n_{\pi_1})$ times `GEMM` with different tensor slices of $\underline{\mathbf{C}}$ and $\underline{\mathbf{A}}$ in the base case. Each `GEMM` computes one slice $\underline{\mathbf{C}}'_{\pi_1,q}$ of the tensor-matrix product $\underline{\mathbf{C}}$ using the corresponding tensor slices $\underline{\mathbf{A}}'_{\pi_1,q}$ and the matrix $\mathbf{B}$. The matrix-matrix product $\mathbf{C} = \mathbf{B} \cdot \mathbf{A}$ is performed by interpreting both tensor slices as matrices $\mathbf{C}$ and $\mathbf{A}$ which have the dimensions (n_{π_1}, m) and (n_q, n_{π_1}), respectively.

4.4 Modified Baseline Algorithms with Adjustable Subtensor Size

Case 1-7 cannot be further optimized. Case 8 uses the modified baseline algorithm 1 to call slice-matrix multiplication.

Enlarge tensor slice and include more modes for the non-contracting mode in order to have slice-matrix multiplications with more elements.

What can be $(1, .., \pi_1, .., q, .., p)$ and $(1, .., q, .., \pi_1, .., p)$

Take $\pi_1, .., q$ and

4.5 Parallel Algorithms with Slice-Vector Multiplications

A straight-forward approach for generating a parallel version of Algorithm **??** is to divide the outer-most π_p-th loop into equally sized iterations and execute them in parallel using the `OpenMP parallel for` directive [4]. With no critical sections and synchronization points, all threads within the parallel region execute their own sequential slice-vector multiplications. The outer-most dimension n_{π_p} determines the degree of parallelism, i.e. the number of parallel threads executing their own instruction stream.

Fusing additional loops into a single one improves the degree of parallelism. The number of fusible loops depends on the tensor order p and contraction mode q of the tensor-vector multiplication with $\hat{q} = (\pi^{-1})_q$. In case of mode-q slice-vector multiplications, loops $\pi_{\hat{q}+1}, \ldots, \pi_p$ are not involved in the multiplications and can be transformed into one single loop. For mode-2 slice-vector multiplications all loops except π_1 and $\pi_{\hat{q}}$ can be fused. When all fusible loops are lexically present and both parameters are known before compile time, loop fusion and parallel execution can be easily accomplished with the `OpenMP collapse` directive. The authors of [10] use this approach to generate parallel tensor-matrix functions.

With variable number of dimensions and a variable contraction mode, the iteration count of slice-vector multiplications and the slice selection needs to be determined at compile or run time. If $\bar{n}$ is the number of tensor elements of $\mathbf{\underline{A}}$, the total number of slice-vector multiplications with mode-$\hat{q}$ slices is given by $\bar{n}' = \bar{n}/w_q$. Using Eq. (**??**), the strides for the iteration are given by $w_{\pi_{\hat{q}+1}}$ for $\mathbf{\underline{A}}$ and $v_{\pi_{\hat{q}}}$ for $\mathbf{\underline{C}}$. In summary, one single parallel outer loop with an iteration count $\bar{n}'$ and an increment variable j iteratively calls mode-$\hat{q}$ slice-vector multiplications with adjusted memory location $j \cdot w_{\pi_{\hat{q}+1}}$ and $j \cdot v_{\pi_{\hat{q}}}$ for $\mathbf{\underline{A}}$ and $\mathbf{\underline{C}}$, respectively. The degree of parallelism $\prod_{r=\hat{q}+1}^{p} n_r$ decreases with increasing $\hat{q}$ and corresponds for $\hat{q} = p-1$ to the first parallel version. Tensor-vector multiplications with mode-2 slice-vector multiplications are further optimized by fusing additional $\hat{q}-2$ loops.

5 Experimental Setup

Computing System The experiments were carried out on a Core i9-7900X Intel Xeon processor with 10 cores and 20 hardware threads running at 3.3 GHz. It has a theoretical peak memory bandwidth of 85.312 GB/s resulting from four 64-bit wide channels with a data rate of 2666MT/s. The sizes of the L3-cache and each L2-cache are 14MB and 1024KB. The source code has been compiled with `GCC v7.3` using the highest optimization level `-Ofast` and `-march=native`, `-pthread` and `-fopenmp`. Parallel execution for the general case (8) has been accomplished

using `GCC`'s implementation of the `OpenMP v4.5` specification. We have used the `DOT` and `GEMV` implementation of the `OpenBLAS` library `v0.2.20`. The benchmark results of each function are the average of 10 runs.

Tensor Shapes We have used *asymmetrically-shaped* and *symmetrically-shaped* tensors in order to provide a comprehensive test coverage. *Setup 1* performs runtime measurements with *asymmetrically-shaped* tensors. Their dimension tuples are organized in 10 two-dimensional arrays $\mathbf{N}_q$ with 9 rows and 32 columns where the dimension tuple $\mathbf{n}_{r,c}$ of length $r+1$ denotes an element $\mathbf{N}_q(r,c)$ of $\mathbf{N}_q$ with $1 \leq q \leq 10$. The dimension $\mathbf{n}_{r,c}(i)$ of $\mathbf{N}_q$ is 1024 if $i = 1$, $c \cdot 2^{15-r}$ if $i = \min(r+1, q)$ and 2 for any other index i with $1 < q \leq 10$. The dimension $\mathbf{n}_{r,c}(i)$ of $\mathbf{N}_1$ is given by $c \cdot 2^{15-r}$ if $i = 1$, 1024 if $i = 2$ and 2 for any other index i. Dimension tuples of the same array column have the same number of tensor elements. Please note that with increasing tensor order (and row-number), the contraction mode is halved and with increasing tensor size, the contraction mode is multiplied by the column number. Such a setup enables an orthogonal test-set in terms of tensor elements ranging from 2^{25} to 2^{29} and tensor order ranging from 2 to 10. *Setup 2* performs runtime measurements with *symmetrically-shaped* tensors. Their dimension tuples are organized in one two-dimensional array $\mathbf{M}$ with 6 rows and 8 columns where the dimension tuple $\mathbf{m}_{r,c}$ of length $r+1$ denotes an element $\mathbf{M}(r,c)$ of $\mathbf{M}$. For $c = 1$, the dimensions of $\mathbf{m}_{r,c}$ are given by 2^{12}, 2^8, 2^6, 2^5, 2^4 and 2^3 with descending row number r from 6 to 1. For $c > 1$, the remaining dimensions are given by $\mathbf{m}_{r,c} = \mathbf{m}_{r,c} + k \cdot (c-1)$ where k is 2^9, 2^5, 2^3, 2^2, 2, 1 with descending row number r from 6 to 1. In this setup, shape tuples of a column do not yield the same number of subtensor elements.

Performance Maps Measuring a single tensor-vector multiplication with the first setup produces $2880 = 9 \times 32 \times 10$ runtime data points where the tensor order ranges from 2 to 10, with 32 shapes for each order and 10 contraction modes. The second setup produces $336 = 6 \times 8 \times 7$ data points with 6 tensor orders ranging from 2 to 7, 8 shapes for each order and 7 contraction modes. Similar to the findings in [4], we have observed a performance loss for small dimensions of the mode with the highest priority. The presented performance values are the arithmetic mean over the set of tensor sizes that vary with the tensor order and contraction mode resulting in a three dimensional performance plot. A schematic countour view of the plots is given in Fig. 1 which is divided into 5 regions. The cases 2, 3, 6 and 7 generate performance values within the regions 2, 3, 6 and 7 where only a single parallel `GEMV` is executed, see Table 1. Please note that the contraction mode q is set to the tensor order p if $q > p$. Performance values within region 8 result from case 8 which executes `GEMV`'s with tensor slices in parallel.

The following analysis considers four parallel versions `SB-P1`, `LB-P1`, `SB-PN` and `LB-PN`. `SB` (small-block) and `LB` (large-block) denote parallel slice-vector multiplications where each thread recursively calls a single-threaded `GEMV` with mode-2 and mode-$\hat{q}$ slices, respectively. `P1` uses the outer-most dimension n_p for parallel
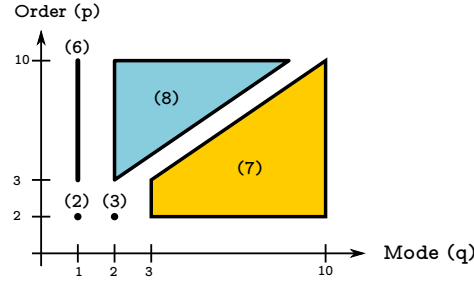
Fig. 1. Schematic contour view of the following average performance maps for the tensor-vector multiplication with tensors that are stored according to the first-order storage format. Each case x in Table 1 affects a different region x within the performance map. Performance values are the arithmetic mean over the set of tensor sizes with 32 and 8 elements in case of the first and second test setup, respectively. Contraction mode $q = p$ for $q > p$ where p is the tensor order.

execution whereas `PN` applies loop fusion and considers all fusible dimensions for parallel execution.

6   Results and Discussion

Matrix-Vector Multiplication Fig. 2 shows average performance values of the four versions `SB-P1`, `LB-P1`, `SB-PN` and `LB-PN` with asymmetrically-shaped tensors. In case 2 (region 2), the shape tuple of the two-order tensor is equal to (n_2, n_1) where n_2 is set to 1024 and n_1 is $c \cdot 2^{14}$ for $1 \leq c \leq 32$. In case 6 (region 6), the p-order tensor is interpreted as a matrix with a shape tuple $(\bar{n}_1, n_1)$ where n_1 is $c \cdot 2^{15-r}$ for $1 \leq c \leq 32$ and $2 < r < 10$. The mean performance averaged over the matrix sizes is around 30 Gflops/s in single-precision for both cases. When $p = 2$ and $q > 1$, all functions execute case 3 with a single parallel `GEMV` where the 2-order tensor is interpreted as a matrix in column-major format with a shape tuple (n_1, n_2). In this case, the performance is 16 Gflops/s in region 3 where the first dimension of the 2-order tensor is equal to 1024 for all tensor sizes. The performance of `GEMV` increases in region 7 with increasing tensor order and increasing number of rows $\bar{n}_q$ of the interpreted p-order tensor. In general, `OpenBLAS`'s `GEMV` provides a sustained performance around 31 Gflops/s in single precision for column- and row-major matrices. However, the performance drops with decreasing number of rows and columns for the column-major and row-major format. The performance of case 8 within region 8 is analyzed in the next paragraph.

Slicing and Parallelism Functions with `P1` run with 10 Gflops/s in region 8 when the contraction mode q is chosen smaller than or equal to the tensor order p. The degree of parallelism diminishes for $n_p = 2$ as only 2 threads sequentially execute a `GEMV`. The second method `PN` fuses additional loops and is able to
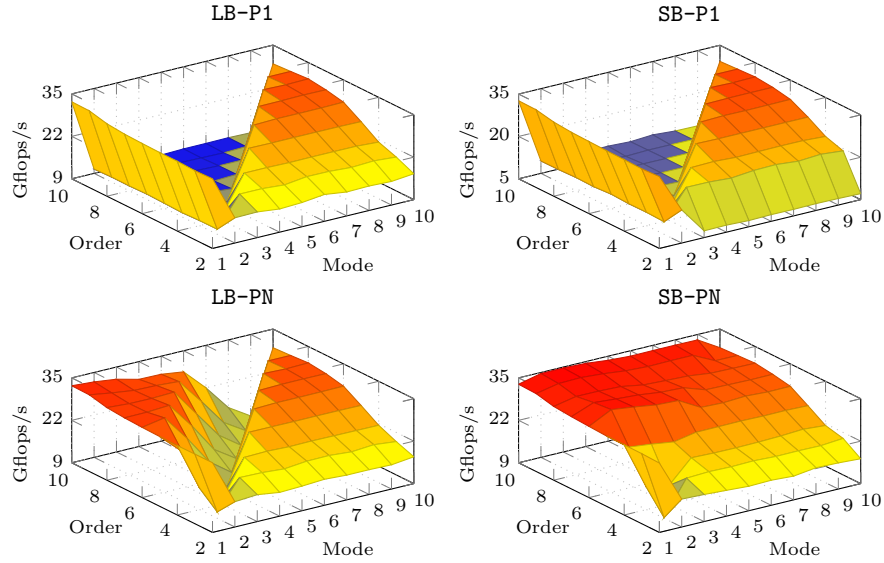
Fig. 2. Average performance maps of four tensor-vector multiplications with varying tensor orders p and contraction modes q. Tensor elements are encoded in single-precision and stored contiguously in memory according to the first-order storage format. Tensors are *asymmetrically-shaped* with dimensions.

generate a higher degree of parallelism. Using the first-order storage format, the outer dimensions $n_{q+1}, \ldots, n_p$ are executed in parallel. The `PN` version speeds up the computation by almost a factor of 4x except for $q = p - 1$. This explains the notch in the left-bottom plot when $q = p - 1$ and $n_p = 2$.

In contrast to the `LB` slicing method, `SB` is able to additionally fuse the inner dimensions with their respective indices $2, 3, \ldots, p - 2$ for $q = p - 1$. The performance drop of the `LB` version can be avoided, resulting in a degree of parallelism of $\prod_{r=2}^{p} n_r / n_q$. Executing that many small slice-vector multiplications with a `GEMV` in parallel yields a mean peak performance of up to $34.8(15.5)$ Gflops/s in single(double) precision. Around 60% of all 2880 measurements exhibit at least 32 Gflops/s that is `GEMV`'s peak performance in single precision. In case of symmetrically-shaped tensors, both approaches achieve similar results with almost no variation of the performance achieving up on average $26(14)$ Gflops/s in single(double) precision.

Tensor Layouts Applying the first setup configuration with asymmetrically-shaped tensors, we have analyzed the effects of the blocking and parallelization strategy. The `LB-PN` version processes tensors with different storage formats, namely the 1-, 2-, 9- and 10-order layout. The performance behavior is almost the same for all storage formats except for the corner cases $q = \pi_1$ and $q = \pi_p$. Even the performance drop for $q = p - 1$ is almost unchanged. The standard
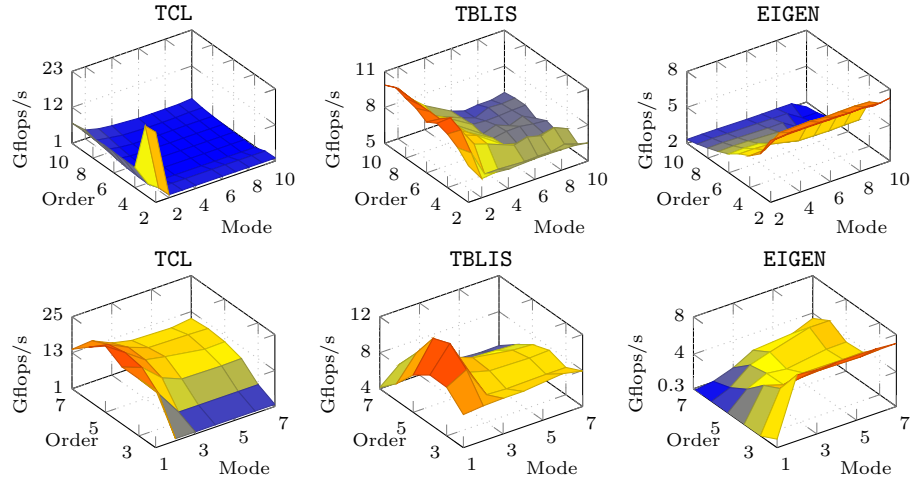

Fig. 3. Average performance maps of tensor-vector multiplication implementations using *asymmetrically-shaped* (top) and *symmetrically-shaped* (bottom) tensors with varying contraction modes and tensor order. Tensor elements are encoded in single-precision and stored contiguously in memory according to the first-order storage format.

deviation from the mean value is less than 10% for all storage formats. Given a contraction mode $q = \pi_k$ with $1 < k < p$, a permutation of the inner and outer tensor dimensions with their respective indices $\pi_1, \ldots, \pi_{k-1}$ and $\pi_{k+1}, \ldots, \pi_p$ does influence the runtime where the LB-PN version calls GEMV with the values w_m and n_m. The same holds true for the outer layout tuple.

Comparison with other Approaches The following comparison includes three state-of-the-art libraries that implement three different approaches. The library TCL (v0.1.1) implements the (TTGT) approach with a high-perform tensor-transpose library HPTT which is discussed in [17]. TBLIS (v1.0.0) implements the GETT approach that is akin to BLIS's algorithm design for matrix computations [12]. The tensor extension of EIGEN (v3.3.90) is used by the Tensorflow framework and performs the tensor-vector multiplication in-place and in parallel with contiguous memory access [1]. TLIB denotes our library that consists of sequential and parallel versions of the tensor-vector multiplication. Numerical results of TLIB have been verified with the ones of TCL, TBLIS and EIGEN.

Fig. 3 illustrates the average single-precision Gflops/s with asymmetrically- and symmetrically-shaped tensors in the first-order storage format. The runtime behavior of TBLIS and EIGEN with asymmetrically-shaped tensors is almost constant for varying tensor sizes with a standard deviation ranging between 2% and 13%. TCL shows a different behavior with 2 and 4 Gflops/s for any order $p \geq 2$ peaking at $p = 10$ and $q = 2$. The performance values however deviate from the mean value up to 60%. Computing the arithmetic mean over the set of contraction modes yields a standard deviation of less than 10% where the
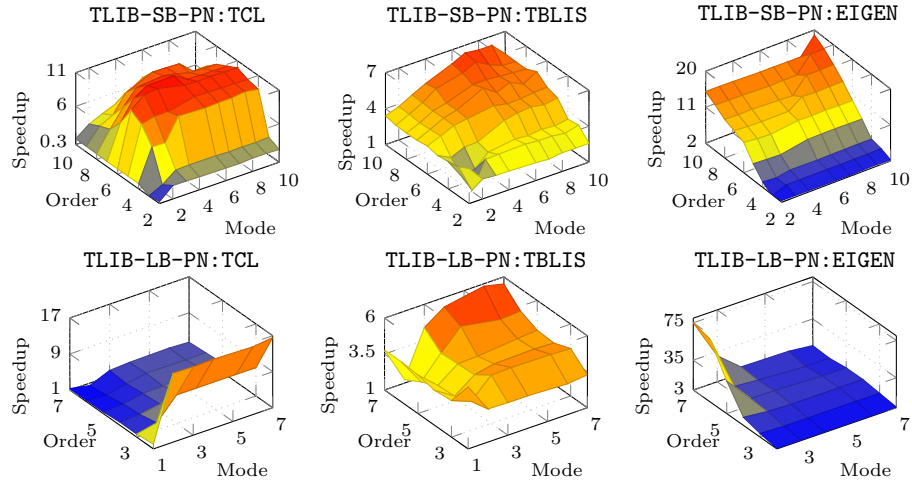
Fig. 4. Relative average performance maps of tensor-vector multiplication implementations using *asymmetrically* (top) and *symmetrically* (bottom) shaped tensors with varying contraction modes and tensor order. Relative performance (speedup) is the performance ratio of `TLIB-SB-PN` (top) and `TLIB-LB-PN` (bottom) to `TBLIS`, `TCL` and `EIGEN`, respectively. Tensor elements are encoded in single-precision and stored contiguously in memory according to the first-order storage format.

performance increases with increasing order peaking at $p = 10$. `TBLIS` performs best for larger contraction dimensions achieving up to 7 Gflops/s and slower runtimes with decreasing contraction dimensions. In case of symmetrically-shaped tensors, `TBLIS` and `TCL` achieve up to 12 and 25 Gflops/s in single precision with a standard deviation between 6% and 20%, respectively. `TCL` and `TBLIS` behave similarly and perform better with increasing contraction dimensions. `EIGEN` executes faster with decreasing order and increasing contraction mode with at most 8 Gflops/s at $p = 2$ and $q \geq 2$.

Fig. 4 illustrates relative performance maps of the same tensor-vector multiplication implementations. Comparing `TCL` performance, `TLIB-SB-PN` achieves an average speedup of 6x and more than 8x for 42% of the test cases with asymmetrically shaped tensors and executes on average 5x faster with symmetrically shaped tensors. In comparison with `TBLIS`, `TLIB-SB-PN` computes the tensor-vector product on average 4x and 3.5x faster for asymmetrically and symmetrically shaped tensors, respectively.

7 Conclusion and Future Work

Based on the `LOG` approach, we have presented in-place and parallel tensor-vector multiplication algorithms of `TLIB`. Using highly-optimized `DOT` and `GEMV` routines of `OpenBLAS`, our proposed algorithms is designed for dense tensors with arbitrary order, dimensions and any non-hierarchical storage format. `TLIB`'s algo-

rithms either directly call `DOT`, `GEMV` or recursively perform parallel slice-vector multiplications using `GEMV` with tensor slices and fibers.

Our findings show that loop-fusion improves the performance of `TLIB`'s parallel version on average by a factor of 5x achieving up to 34.8/15.5 Gflops/s in single/double precision for asymmetrically shaped tensors. With symmetrically shaped tensors resulting in small contraction dimensions, the results suggest that higher-order slices with larger dimensions should be used. We have demonstrated that the proposed algorithms compute the tensor-vector product on average 6.1x and up to 12.6x faster than the `TTGT`-based implementation provided by `TCL`. In comparison with `TBLIS`, `TLIB` achieves speedups on average of 4.0x and at most 10.4x. In summary, we have shown that a `LOG`-based tensor-vector multiplication implementation can outperform current implementations that use a `TTGT` and `GETT` approaches.

In the future, we intend to design and implement the tensor-matrix multiplication with the same requirements also supporting tensor transposition and subtensors. Moreover, we would like to provide an in-depth analysis of `LOG`-based implementations of tensor contractions with higher arithmetic intensity.

Project and Source Code Availability `TLIB` has evolved from the Google Summer of Code 2018 project for extending `Boost`'s uBLAS library with tensors. Project description and source code can be found at https://github.com/bassoy/ttv. The sequential tensor-vector multiplication of `TLIB` is part of `uBLAS` and in the official release of `Boost v1.70.0`.

References

1. Abadi, M., Barham, P., Chen, J., Chen, Z., Davis, A., Dean, J., Devin, M., ..., Zheng, X.: Tensorflow: A system for large-scale machine learning. In: Proceedings of the 12th USENIX Conference on Operating Systems Design and Implementation. pp. 265–283. OSDI'16, USENIX Association, Berkeley, CA, USA (2016)
2. Bader, B.W., Kolda, T.G.: Algorithm 862: Matlab tensor classes for fast algorithm prototyping. ACM Trans. Math. Softw. **32**, 635–653 (December 2006)
3. Bassoy, C.: Design of a high-performance tensor-vector multiplication with blas. In: International Conference on Computational Science. pp. 32–45. Springer (2019)
4. Bassoy, C., Schatz, V.: Fast higher-order functions for tensor calculus with tensors and subtensors. In: International Conference on Computational Science. pp. 639–652. Springer (2018)
5. Golub, G.H., Van Loan, C.F.: Matrix Computations. JHU Press, 4 edn. (2013)
6. Goto, K., Geijn, R.A.v.d.: Anatomy of high-performance matrix multiplication. ACM Transactions on Mathematical Software (TOMS) **34**(3) (2008)
7. Karahan, E., Rojas-López, P.A., Bringas-Vega, M.L., Valdés-Hernández, P.A., Valdes-Sosa, P.A.: Tensor analysis and fusion of multimodal brain images. Proceedings of the IEEE **103**(9), 1531–1559 (2015)

8. Kolda, T.G., Bader, B.W.: Tensor decompositions and applications. SIAM review **51**(3), 455–500 (2009)
9. Lee, N., Cichocki, A.: Fundamental tensor operations for large-scale data analysis using tensor network formats. Multidimensional Systems and Signal Processing **29**(3), 921–960 (2018)
10. Li, J., Battaglino, C., Perros, I., Sun, J., Vuduc, R.: An input-adaptive and in-place approach to dense tensor-times-matrix multiply. In: High Performance Computing, Networking, Storage and Analysis, 2015 SC-International Conference for. pp. 1–12. IEEE (2015)
11. Lim, L.H.: Tensors and hypermatrices. In: Hogben, L. (ed.) Handbook of Linear Algebra. Chapman and Hall, 2 edn. (2017)
12. Matthews, D.A.: High-performance tensor contraction without transposition. SIAM Journal on Scientific Computing **40**(1), C1–C24 (2018)
13. Napoli, E.D., Fabregat-Traver, D., Quintana-Ortí, G., Bientinesi, P.: Towards an efficient use of the blas library for multilinear tensor contractions. Applied Mathematics and Computation **235**, 454 – 468 (2014)
14. Papalexakis, E.E., Faloutsos, C., Sidiropoulos, N.D.: Tensors for data mining and data fusion: Models, applications, and scalable algorithms. ACM Transactions on Intelligent Systems and Technology (TIST) **8**(2), 16 (2017)
15. Shi, Y., Niranjan, U.N., Anandkumar, A., Cecka, C.: Tensor contractions with extended blas kernels on cpu and gpu. In: 2016 IEEE 23rd International Conference on High Performance Computing (HiPC). pp. 193–202 (Dec 2016)
16. Solomonik, E., Matthews, D., Hammond, J., Demmel, J.: Cyclops tensor framework: Reducing communication and eliminating load imbalance in massively parallel contractions. In: Parallel & Distributed Processing (IPDPS), 2013 IEEE 27th International Symposium on. pp. 813–824. IEEE (2013)
17. Springer, P., Bientinesi, P.: Design of a high-performance gemm-like tensor–tensor multiplication. ACM Transactions on Mathematical Software (TOMS) **44**(3), 28 (2018)